

Reaction Cross-Sections and Nuclear Radii in the Quantum Molecular Dynamical Approach

Tomoyuki Maruyama

College of Bioresource Sciences, Nihon University

Abstract

We make a new formulation of the QMD approach, which can give correct mean-square radii for initial nuclei. Then the reaction cross-sections are calculated with various energy region. We succeed to reproduce experimental data even below 100 MeV/u nicely.

The measurement of the ininteraction cross-section (σ_I) at relativistic energy must be a good tool to determine radii of anomalous nuclei as well as normal nuclei. By combining this measurement with the Glauber calculation, furthermore, we will get information of density-distribution of anomalous nuclei, such as halo and skin structures. This method is, however, satisfied only for collisions above several hundred MeV/u, where the elementary NN cross-section does not have strong energy-dependence, and the trajectory of a projectile nucleus is well approximate to be straight.

On the other hand we need to make theoretical analysis of experimental results with the beam energy below 100 MeV/u, where a lot of data is available from RIKEN. In this calculation we must consider effects of energy-dependence of the NN cross-section and curved trajectory of initial nuclei in reaction around 50-100 MeV/u energy region.

Recently we developed a framework of QMD [1] plus statistical decay model (SDM) [2], and applied systematically this QMD + SDM to nucleon- (N-) induced reactions. It was shown [2] that this framework could reproduce quite well the measured double-differential cross-sections of (N,xN') type reactions from 100 MeV to 3 GeV incident energies in a systematic way. In the subsequent papers [3, 4], we gave detailed analysis of the pre-equilibrium (p,xp') and (p,xn) reactions in terms of the QMD in the energy region of 100 to 200 MeV. In these analysis, a single set of parameters was used, and no readjustment was attempted.

In this work we make initial nuclei with correct root-mean-square radii while one has not carefully treated them, and examine reaction cross-sections with the QMD approach in several kinds of energy region.

Now we briefly explain our formulation.

In the QMD, each nucleon state is represented by a Gaussian wave-function of width L ,

$$\phi_i(\mathbf{r}) = \frac{1}{(2\pi L)^{3/4}} \exp \left[-\frac{(\mathbf{r} - \mathbf{R}_i)^2}{4L} + \frac{i}{\hbar} \mathbf{r} \cdot \mathbf{P}_i \right], \quad (1)$$

where \mathbf{R}_i and \mathbf{P}_i are the centers of position and momentum of i -th nucleon, respectively. The total wave-function is assumed to be a direct product of these wave-functions. Thus the

one-body distribution function is obtained by the Wigner transform of the wave-function,

$$f(\mathbf{r}, \mathbf{p}) = \sum_i f_i(\mathbf{r}, \mathbf{p}), \quad (2)$$

$$f_i(\mathbf{r}, \mathbf{p}) = 8 \cdot \exp \left[-\frac{(\mathbf{r} - \mathbf{R}_i)^2}{2L} - \frac{2L(\mathbf{p} - \mathbf{P}_i)^2}{\hbar^2} \right]. \quad (3)$$

The equation of motion of \mathbf{R}_i and \mathbf{P}_i is given by the Newtonian equation

$$\dot{\mathbf{R}}_i = \frac{\partial H_{QMD}}{\partial \mathbf{P}_i}, \quad \dot{\mathbf{P}}_i = -\frac{\partial H_{QMD}}{\partial \mathbf{R}_i}, \quad (4)$$

and the stochastic N-N collision term. Hamiltonian H consists of the kinetic energy and the energy of the two-body effective interaction.

The Hamiltonian is separated into several parts as follows.

$$H_{QMD} = T + V_{\text{Pauli}} + V_{\text{local}} + V_{\text{MD}} + V_{\text{Coulomb}} \quad (5)$$

where T , V_{Pauli} , V_{local} and V_{MD} are the kinetic energy, the Pauli potential, the local (momentum-independent) potential and the momentum-dependent potential parts, respectively.

The Pauli potential [5, 6, 7, 8] is introduced for the sake of simulating the Fermionic property in a semiclassical way. This phenomenological potential prohibits nucleons of the same spin σ and isospin τ from coming close to each other in the phase space. Here we employ the Gaussian form of the Pauli potential [6] as

$$V_{\text{Pauli}} = \frac{1}{2} C_P \left(\frac{\hbar}{q_0 p_0} \right)^3 \sum_{i,j(\neq i)} \exp \left[-\frac{(\mathbf{R}_i - \mathbf{R}_j)^2}{2q_0^2} - \frac{(\mathbf{P}_i - \mathbf{P}_j)^2}{2p_0^2} \right] \delta_{\tau_i \tau_j} \delta_{\sigma_i \sigma_j}. \quad (6)$$

For the convenience of the explanation we separate the local potential part into the Coulomb force, the Skyrme type force with the symmetry terms and the Gaussian force.

$$V_{\text{local}} = V_{\text{Sky}} + V_{\text{Sym}} + V_G \quad (7)$$

The V_{Sky} and the V_{Sym} describe the zero range nuclear force whose detailed form is given as

$$\begin{aligned} V_{\text{Sky}} &= \frac{\alpha}{2\rho_0} \sum_i \langle \rho_i \rangle + \frac{\beta}{(1+\tau)\rho_0^\tau} \sum_i \langle \rho_i \rangle^\tau \\ V_{\text{Sym}} &= \frac{C_s}{2\rho_0} \sum_{i,j(\neq i)} (1 - 2|c_i - c_j|) \rho_{ij} \end{aligned} \quad (8)$$

with

$$\begin{aligned} \langle \rho_i \rangle &\equiv \sum_{j \neq i} \rho_{ij} \equiv \sum_{j \neq i} \int d^3r \rho_i(\mathbf{r}) \rho_j(\mathbf{r}) \\ &= \sum_{j \neq i} (4\pi L)^{-3/2} \exp \left[-(\mathbf{R}_i - \mathbf{R}_j)^2 / 4L \right], \end{aligned} \quad (9)$$

To describe the finite range nuclear interaction the Yukawa force is often used, but it consumes a rather long CPU time. Instead of that we take the Gaussian force V_G as

$$V_G = \frac{\alpha_G}{2\rho_0} \sum_i \langle g_i \rangle \quad (10)$$

Table 1: Effective interaction parameter set

α (MeV)	-1.00
β (MeV)	188.42.
τ	1.33333
α_G (MeV)	-107.52
C_s (MeV)	-258.54
$C_{\text{ex}}^{(1)}$ (MeV)	-258.54
$C_{\text{ex}}^{(2)}$ (MeV)	375.6
μ_1 (MeV)	2.35
μ_2 (MeV)	0.4
L (fm ²)	1.2
L_g (fm ²)	2.0
q_0 (fm)	2.0
p_0 (MeV)	100.0
C_p (MeV)	53.5

with

$$\begin{aligned}
\langle g_i \rangle &\equiv \sum_{j \neq i} g_{ij} \equiv \sum_{j \neq i} \int d^3r d^3r' \rho_i(\mathbf{r}) (4\pi\gamma_g)^{-3/2} \exp\left[-(\mathbf{r} - \mathbf{r}')^2/4\gamma_g\right] \rho_j(\mathbf{r}') \\
&= \sum_{j \neq i} (4\pi L_g)^{-3/2} \exp\left[-(\mathbf{R}_i - \mathbf{R}_j)^2/4L_g\right],
\end{aligned} \tag{11}$$

where

$$L_g = 2L + \gamma_g \tag{12}$$

The momentum-dependent term is introduced as a Fock term of the Yukawa-type interaction. We divide this interaction into two ranges so as to fit the effective mass and the energy dependence of the real part of the optical potential [11]:

$$\begin{aligned}
V_{\text{MD}} &= V_{\text{MD}}^{(1)} + V_{\text{MD}}^{(2)} \\
&= \frac{C_{\text{ex}}^{(1)}}{2\rho_0} \sum_{i,j(\neq i)} \frac{1}{1 + \left[\frac{\mathbf{P}_i - \mathbf{P}_j}{\mu_1}\right]^2} \rho_{ij} + \frac{C_{\text{ex}}^{(2)}}{2\rho_0} \sum_{i,j(\neq i)} \frac{1}{1 + \left[\frac{\mathbf{P}_i - \mathbf{P}_j}{\mu_2}\right]^2} \rho_{ij}.
\end{aligned} \tag{13}$$

In the above expression we have fourteen parameters $V_p, q_0, P_0, \alpha, \beta, \tau, \alpha_g, C_s, V_{MD}^{(1)}, V_{MD}^{(2)}, \Lambda_1, \Lambda_2$ and the Gaussian width L and L_g . We parametrized their values to reproduce properties of the ground state and the energy-dependence of the empirical proton-nucleus optical potential; in Table 1 we give a parameter-set

In our method we do not define the ground state of nuclei as a energy minimum state of the system, while in a usual method they get the initial distribution by searching the energy minimum state with the frictional cooling method [5]. The other parameters are determined to reproduce properties of finite nuclei as follows. To get the initial nuclear distribution we first distribute the particles randomly in phase space and cool down the system according to the damping equation of motion until the energy reaches the experimental value. Then we

examine its stability by evaluating equations of motion for initial nucleons until 500 fm/c. We determine the parameters of the mean-fields to root-mean-square radii of various nuclei, which are calculated by averaging events and several time steps, when the binding energies agree with the experimental value. Here the Pauli potential is determined to give a averaged kinetic energy 25 MeV for ^{40}Ca .

Fig. 1 shows calculation results of time-averaging root-mean-square radii of several nuclei, whose binding energies are given as experimental data.

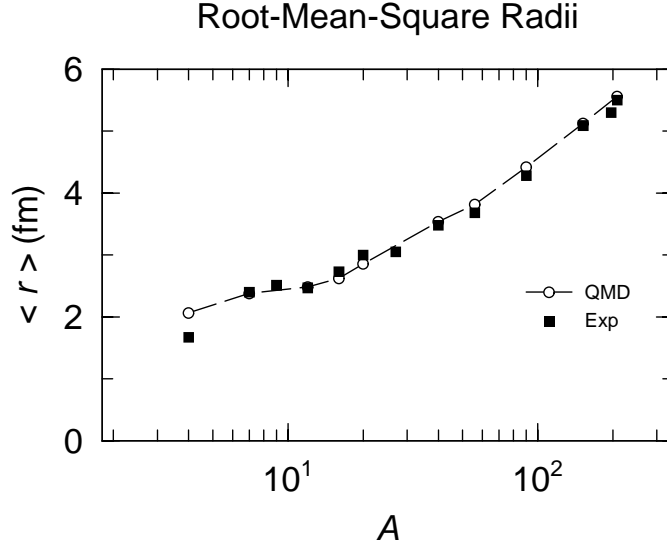


Fig. 1: Time averaging root-mean-square radius of ground state nuclei. Open circles show the results of QMD and the full squares indicate experimental results.

In Fig. 2 we show the time-dependence of the root-mean-square radii in one event. We can see that the fluctuation is not so large in the time evolution.

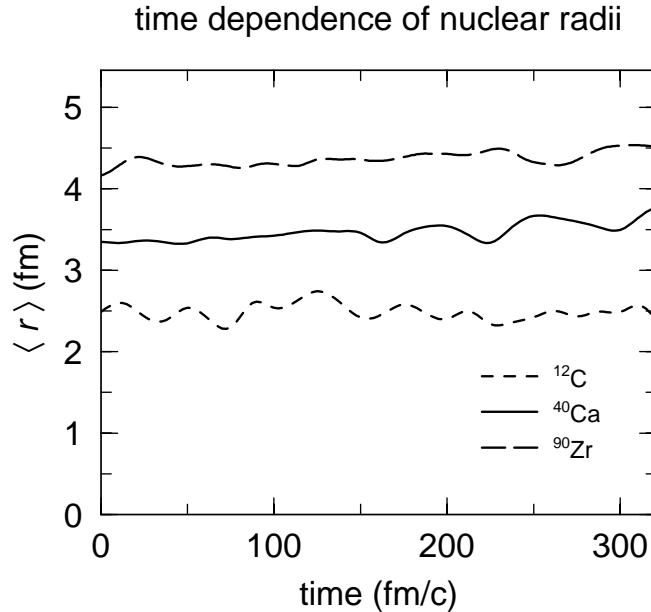


Fig. 2: Time dependence of root-mean-square radii of ^{12}C (dashed line), ^{40}Ca (solid line), ^{90}Zr (solid line).

As a next step we calculate energy-dependence of reaction cross-sections in the QMD approach. We define a reaction event where one NN collision occurs, and evaluate the reaction cross-section by summing reaction probabilities for all impact-parameters.

For the collision judgment including the Gaussian width we use the possibility given by the following equation

$$\frac{1}{(2\pi L)^3} \int d^3x d^3y \theta\{b_{coll} - |\mathbf{x}_T - \mathbf{y}_T|\} \exp\left[-\frac{(\mathbf{x} - \mathbf{R}_i)^2 + (\mathbf{y} - \mathbf{R}_j)^2}{2L}\right], \quad (14)$$

where θ is the step function, and b_{coll} is given from the total NN cross-section as

$$\sigma_T = \pi b_{coll}^2 \quad (15)$$

with the NN collision cross-section σ_T experimentally observed.

In Fig. 3 we draw target-mass-number dependence of reaction cross-sections for the carbon beam at 83 MeV/u and 300 MeV/u. We can see that the QMD approach nicely reproduce experimental results [9] even below 100 MeV/u. Then we can conclude that our approach is effective for the present purpose.

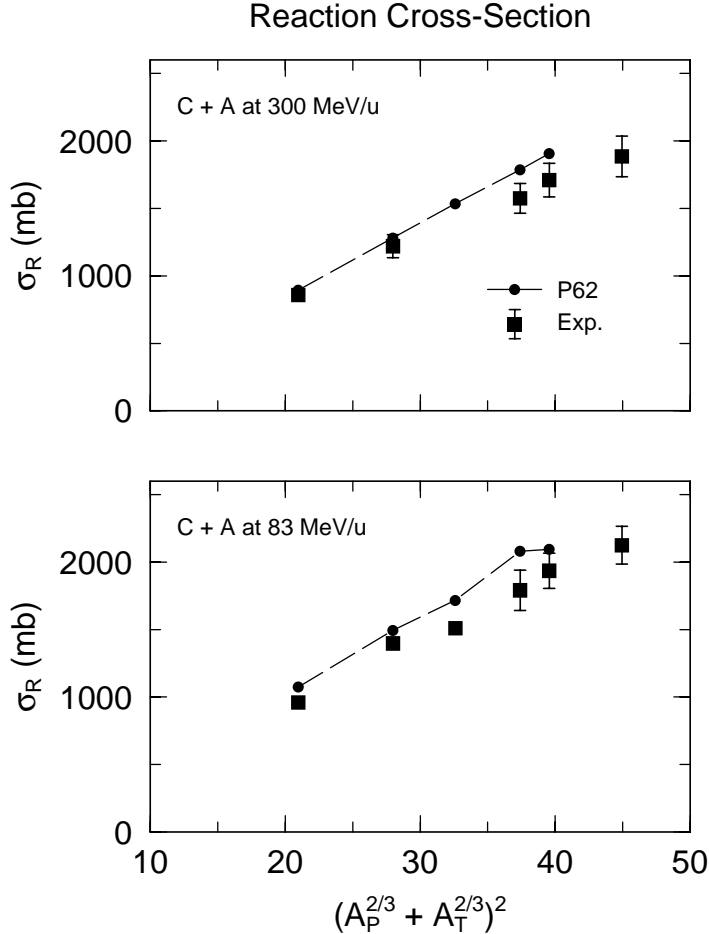


Fig. 3: Target-mass dependence of the reaction cross-sections of collisions with the carbon beam at the incident energies 300 MeV/u (upper column) and 83 MeV/u (lower column). Experimental data (squares) are taken from Ref. [9].

In summary we make a new QMD formulation to give correct root-mean-square radii

for stable nuclei, and calculate the reaction cross-sections in several energy region. We will succeed to reproduce experimental data up to about 80 MeV. Now we are testing reactions with isotope beams. After that we will extend this approach to control initial distribution and to determine the radii of exotic nuclei.

References

- [1] J. Aichelin, Phys. Rep. **202**, 233 (1991), and references therein.
- [2] K. Niita, S. Chiba, T. Maruyama, T. Maruyama, H. Takada, T. Fukahori, Y. Nakahara and A. Iwamoto, Phys. Rev. C **52**, 2620 (1995).
- [3] M. B. Chadwick, S. Chiba, K. Niita, T. Maruyama and A. Iwamoto, Phys. Rev. C **52**, 2800 (1995); S. Chiba, M. B. Chadwick, K. Niita, T. Maruyama and A. Iwamoto, Phys. Rev. C **53**, 1824 (1996); S. Chiba, O. Iwamoto, T. Fukahori, K. Niita, T. Maruyama, T. Maruyama and A. Iwamoto, Phys. Rev. C **54**, 285 (1996).
- [4] S. Chiba, M.B. Chadwick, K.Niita, T. Maruyama, T. Maruyama and A. Iwamoto, Phys. Rev. C **53**, 1824 (1996).
- [5] T. Maruyama, K Niita, K. Oyamatsu, T. Maruyama, S. Chiba, A. Iwamoto, Phys. Rev. C **57** 655.
- [6] G. Peilert, J. Konopka, H. Stöcker, W. Greiner, M. Blann and M. G. Mustafa, Phys. Rev. C **46** (1992) 1457.
- [7] D. H. Boal and J. N. Glosli, Phys. Rev. C **38** (1988) 1870.
- [8] A. Ohnishi, T. Maruyama and H. Horiuchi, Prog. Theor. Phys. **87** (1992) 417.
- [9] S. Kox, et al.: Phys. ReV. C **35**, 1678 (1987).
- [10] D. G. Ravenhall, C. J. Pethick and J. R. Wilson, Phys. Rev. Lett. **27** (1983) 2066.
- [11] S. Hama, B. C. Clark, E. D. Cooper, H. S. Scherif and R. L. Mercer, Phys. Rev. C **41** (1990) 2737.